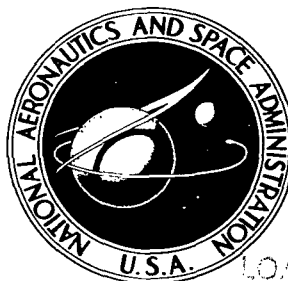


NASA TECHNICAL NOTE



NASA TN D-2792

NASA TN D-2792

LOAN COPY: RETUR
AFWL (WLIL-2)
KIRTLAND AFB, N M



AN APPROXIMATE DETERMINATION OF THE EFFECTS OF GEOMETRY ON BALL-BEARING TORQUE AND FATIGUE LIFE

by John T. Mayer and Thomas C. Litzler

Lewis Research Center

Cleveland, Ohio





AN APPROXIMATE DETERMINATION OF THE EFFECTS OF GEOMETRY
ON BALL-BEARING TORQUE AND FATIGUE LIFE

By John T. Mayer and Thomas C. Litzler

Lewis Research Center
Cleveland, Ohio

NATIONAL AERONAUTICS AND SPACE ADMINISTRATION

For sale by the Clearinghouse for Federal Scientific and Technical Information
Springfield, Virginia 22151 - Price \$1.00

AN APPROXIMATE DETERMINATION OF THE EFFECTS OF GEOMETRY ON BALL-BEARING TORQUE AND FATIGUE LIFE

by John T. Mayer and Thomas C. Litzler

Lewis Research Center

SUMMARY

Existing theoretical analyses were used to calculate ball-spin torque and fatigue life of thrust-loaded ball bearings over a wide range of load, speed, and bearing geometric parameters. The aim of this study was to quantitatively determine the effects of bearing geometry on ball-spin torque and life and to establish design criteria with regard to geometry for rocket turbopump bearings. The following variables were examined for their effect on ball-spin torque and life: contact angle, race curvature, ball size and number, and pitch diameter.

Calculations were performed for several bearing geometries corresponding to 50-, 100-, and 150-millimeter bore sizes. The load and speed ranges examined were 1000 to 10 000 pounds and 10 000 to 25 000 rpm, respectively.

Results indicated that minor changes in standard bearing geometries can greatly alter torque and fatigue life, and that in some cases a particular change can improve the bearing in both of these operational aspects. Race curvature and ball size had the most pronounced effects on torque and life. Although most geometry changes that reduced torque also reduced fatigue life, a certain degree of optimization can be achieved. General rules were outlined for such an optimization.

INTRODUCTION

In recent years there has been an increase in the use of rolling element bearings operating in cryogenic fluids. This is especially true in rocket turbopump systems, where the ball and roller bearings are directly lubricated and cooled by the cryogenic propellants, which at best provide marginal lubrication. Weight and complexity can be reduced by eliminating the conventional lubrication system from the turbopump, however,

the high loads and speeds imposed result in high heat generation rates within the bearings. In order to remove this heat and maintain an equilibrium temperature condition within the bearing, it may be necessary to improve the cooling efficiency of the cryogenic fluid by pressure feeding it through the bearing. The heat balance is sometimes difficult to maintain, especially when the bearing must survive at such severe operating conditions. The result is loss of internal clearance and ultimate bearing seizure. Excessive heat generation is one of the most important problems in cryogenic bearing development. Other problem areas include lubrication mechanisms, materials, retainer design, rolling-contact fatigue and, in the case of nuclear rockets, radiation damage.

Much has been accomplished toward improving the operation of bearings in fluids such as liquid hydrogen and oxygen. The main effort has been directed toward alleviating the heat generation problem. Two more common approaches used are (1) reduction of bearing friction by providing an internal self-lubricating mechanism and (2) control of the heat generation by improving the cooling efficiency. A certain degree of success has been realized in the areas of solid lubrication and cage design, but in many cases the problem is only partially solved.

For the case of high speed, thrust-loaded ball bearings, one important source of torque or heat generation is the spinning motion of the balls at the race contacts. This portion of the total bearing torque can be calculated by using existing analyses and is found to be directly related to the bearing's internal geometry. Thus, it is possible to further reduce heat generation by an appropriate choice of bearing geometric parameters. The investigation of the effects of bearing geometry on ball-spin torque has not been very extensive, either experimentally or analytically. Experimental studies have been limited to higher rotative speeds and moderate thrust loads (ref. 1). As for analytical studies, very little quantitative information has been published (refs. 1 and 2) and that which is available cannot be expected to pertain to all bearing sizes, loads, and speeds. In addition, nothing has been done to correlate the effects of bearing geometry on fatigue life, which can be a limiting factor in torque reduction. Contrastingly, changes in geometry that are beneficial with regard to ball-spin torque are often detrimental to fatigue life. It is desirable, therefore, that both aspects be studied.

The purpose of the work described in this report was to examine the effects of certain bearing geometric parameters on ball-spin torque and fatigue life by using existing analyses. The specific aim was to establish design criteria with respect to ball-bearing geometry for nuclear rocket hydrogen turbopump applications. Although the main interest was in minimizing ball-spin torque, a less extensive study of fatigue life was also made because of its secondary importance as a limiting factor.

The variables examined for their effect on ball-spin torque and fatigue life were: initial contact angle, ball size, number of balls, pitch diameter, and race curvatures. In order to provide data for both present and future hydrogen pump designs, three bore

sizes were examined (50, 100, and 150 mm) over a speed range of 10 000 to 25 000 rpm. An empirical expression relating pump horsepower to shaft size and speed (unpublished NASA data), verified that an optimum pump design would be within the bore and speed ranges cited previously. A thrust-load range of 1000 to 2500 pounds was chosen for examination. Realizing that these loads are low for the larger bore sizes, additional data were obtained at 6000 pounds (100-mm bore) and 10 000 pounds (150-mm bore) in order to determine any discrepancies at higher loads.

DESCRIPTION OF THEORY AND METHOD

Ball-Spin Friction Torque

The method used in computing ball-spin torque is that of Scibbe and Anderson (ref. 1). It is based on analyses of ball-bearing forces and motion by Jones (ref. 3) and Poritsky, Hewlett, and Coleman (ref. 4). It is applicable only to ball bearings under pure thrust load. The method of reference 1 provides a means of calculating the torque due to ball spin at the race contacts. It is generally held (e. g., ref. 5) that this is one of the major contributors to the total bearing torque in thrust-carrying ball bearings. In subsequent parts of this report, the torque referred to is the ball-spin friction torque. Other sources of friction such as ball rolling and cage rubbing were not considered in this approximation to the total torque. A further simplification is obtained by assuming that moments arising from the gyroscopic effects of the balls are negligible with respect to the spinning moments. This results in ball "control" at one race; that is, essentially pure rolling occurs at one race, and a combination of spinning and rolling occurs at the other. Calculations showed that a coefficient of friction of 0.1 is sufficient to prevent ball slip due to gyroscopic effects. The location of ball control is determined by the operating conditions and the bearing geometry; control will be at the race where the spinning moment is larger.

The aforementioned method is limited in its range of applicability and involves several approximations. It was judged adequate, however, as a first approximation for the intended application. Although turbopump ball bearings do not generally operate under pure thrust load, the ratio of thrust to radial load is usually high. Thus, it is expected that the effects of radial load on ball-spin torque will be negligible.

In the calculation of torque a value of 0.56 was used for the friction coefficient. This value was measured (ref. 1) for unlubricated 440 C stainless steel sliding on itself in liquid hydrogen. Actually, the precise value is unimportant for this analysis, since ball-spin torque varies linearly with the friction coefficient and only relative changes in torque are of interest.

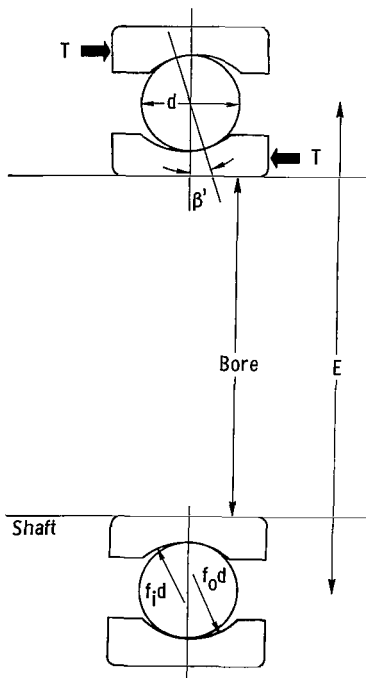


Figure 1. - Bearing parameters.

Symbols are defined in appendix A, while the equations to be solved for the ball-spin friction torque are given in appendix B. These equations have been programed on a digital computer (ref. 1). The input necessary is as follows: number and diameter of the balls, pitch diameter, initial contact angle, race-curvature factors, load, and speed. These variables are illustrated in figure 1. Output from the equations includes the bearing shaft torque due to ball spin and both inner- and outer-race spinning moments.

The range of the input variables was chosen so that the effect of each variable on ball-spin torque could be determined, while the others were held constant. Calculations were made with at least three values each of n , d , and E for each bore size. The values chosen approximated the extra-light or light series geometries. For each (n , d , E) combination used, torque was obtained over the following ranges:

Inner-race speed, N_i , rpm	10 000 to 25 000
Bearing thrust load, T , lb	1000 to 2500
Initial contact angle (unloaded), β' , deg	15, 20
Race-curvature combination, f_o/f_i	At least five values with f ranging from 0.52 to 0.58

In addition, data were obtained for the 100-millimeter bore size at 6000 pounds and 20 000 rpm, and for the 150-millimeter bore size at 10 000 pounds and 15 000 rpm, at the race curvatures and contact angles in the previous list. The bores and speeds involved imply the ranges in DN (the product of shaft speed in rpm and bore in mm) given in table I.

TABLE I. - RANGE OF DN

EXAMINED	
Bearing bore, mm	DN range
50	0.5×10^6 to 1.25×10^6
100	1.0×10^6 to 2.5×10^6
150	1.5×10^6 to 3.75×10^6

Fatigue Life

The standard life equation of Lundberg and Palmgren (ref. 6) is given in equation (B12). It gives L_B (the statistical fatigue life that 90 percent of all bearings tested will exceed) for ball bearings in millions of revolutions. The life as given in this equation is a function of bearing dimensions and load but is independent of speed. The effect of

centrifugal ball loading on the bearing life was included in the life calculations by applying a correction factor derived by Jones (ref. 7) to the Lundberg-Palmgren life equation. This factor gives the ratio of lives with and without centrifugal-load considerations L_{CF}/L_B and is given in equation (B13). The resulting life L_{CF} is also expressed as the 90 percent statistical life and is the life referred to in subsequent parts of this report.

In general, the geometry input used to calculate L_{CF} was the same as that for the friction torque calculations. The load and speed ranges were not as extensive for life, however. The only variables analyzed over the entire load and speed range were contact angle and curvature. The effects of n , d , and E on life were determined only for limited load and speed combinations.

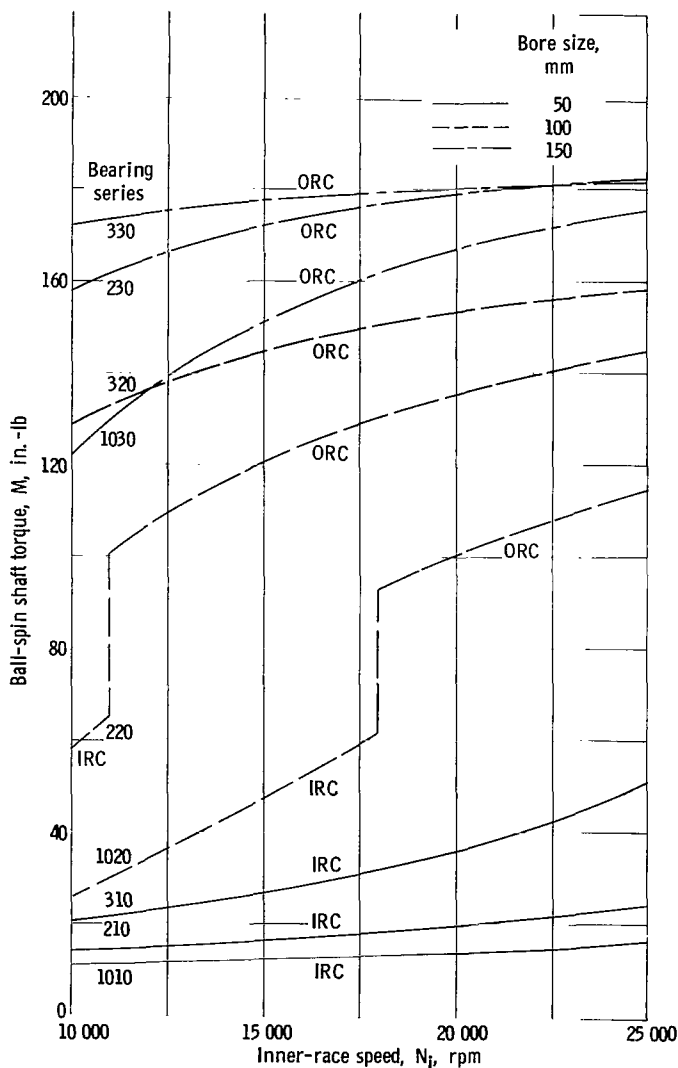


Figure 2 - Torque characteristics of standard series bearings. Initial contact angle (unloaded), 15° ; bearing thrust load, 2500 pounds; race-curvature combination, 0.58/0.52.

RESULTS AND DISCUSSION

Ball-Spin Friction Torque

The discussion of the results of ball-spin torque calculations is in two parts. The first section deals with general variations in torque with load, speed, and bore size. The second section examines the specific effects of each of the five parameters on torque for all load and speed conditions, including the larger load values (6000 and 10 000 lb) for the 100- and 150-millimeter sizes. Although the curves do not cover all the results obtained, they are representative for the range of variables examined.

General results. - The friction torque values of nine standard series bearings are plotted as a function of speed for a constant thrust load (2500 lb) in figure 2 to show general characteristics. The geometries of these standard bearings are listed in table II. Examination of the spinning

TABLE II. - GEOMETRIES OF STANDARD
SERIES BEARINGS

Bearing series number	Bore size, mm	Bearing series name	Number of balls, n	Ball diameter, d, in.	Pitch diameter, E, in.
1010	50	Extra light	18	0.344	2.559
210	50	Light	14	.469	2.755
310	50	Medium	11	.719	3.150
1020	100	Extra light	22	.594	4.920
220	100	Light	14	.969	5.511
320	100	Medium	11	1.375	6.201
1030	150	Extra light	23	.875	7.382
230	150	Light	16	1.375	8.268
330	150	Medium	12	2.125	9.251

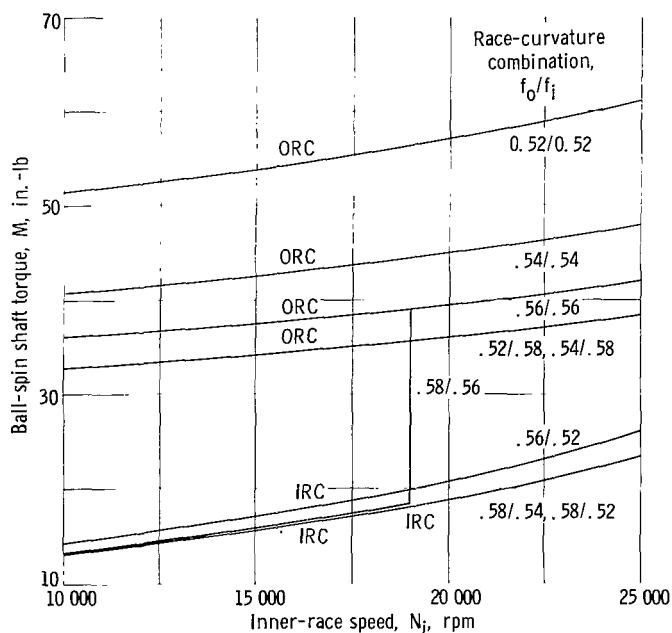


Figure 3. - Effects of curvature on torque. Bore size, 50 millimeters; number of balls, 16; ball diameter, 0.438 inch; pitch diameter, 2.755 inches; initial contact angle (unloaded), 20° ; bearing thrust load, 2500 pounds.

moments $M_{s,i}$ and $M_{s,o}$ showed that control was at the inner race for all 50-millimeter series up to 25 000 rpm and for two of the 100-millimeter series at lower speeds. The 150-millimeter bearings were at outer-race control (ORC) for the entire speed range. The vertical lines for the two 100-millimeter curves represent a transition from inner- to outer-race control. This is the point at which the outer-race spinning moment exceeds the inner. By extrapolating the values of the ball-spinning moments to higher speeds, it was found that a transition also took place for the 50-millimeter bearings, above 25 000 rpm. For any bearing there is a tendency for the outer-race spinning moment to increase with speed. Thus, for a bearing with inner-race control (IRC) at lower speed, control will shift to the outer race at some higher speed. On the other hand, a bearing with ORC will remain so for all higher speeds. The transition speed from IRC to ORC for a particular curvature combination is a function of load as well as bearing geometry. A higher transition speed is obtained when the load is increased, or when the variables n , d , E , or β^* are decreased because these changes contribute to the increasing of the inner-race moment over that of the outer race. It explains why control at the inner race is more difficult to obtain as bore size increases. Larger bore sizes have a greater number of balls, and

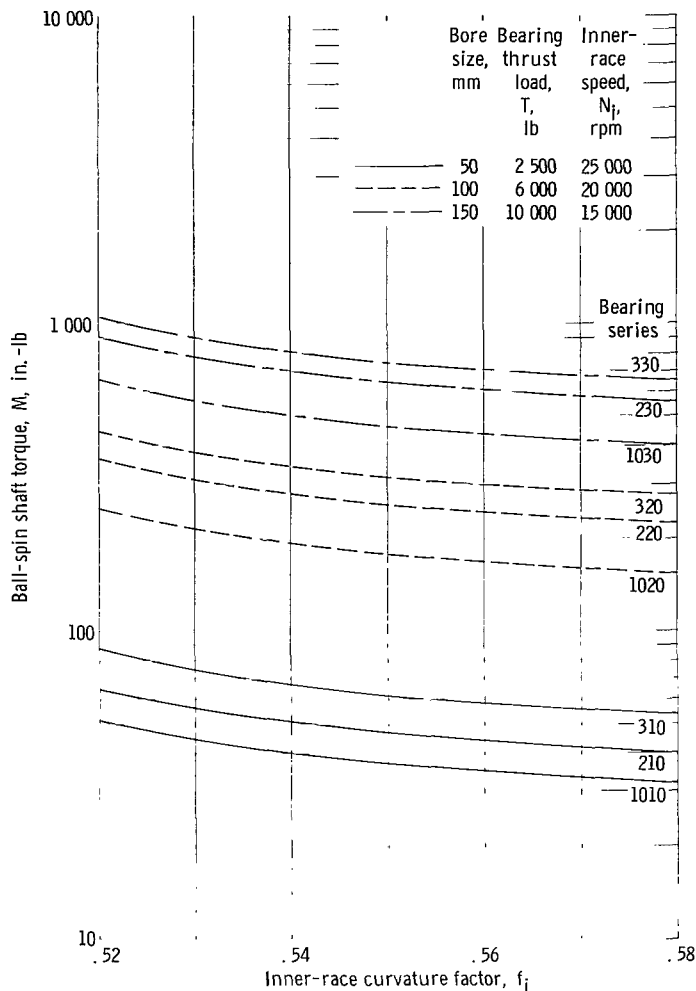


Figure 4. - Effects of curvature on torque for standard bearings at outer-race control. Initial contact angle (unloaded), 20° .

larger ball and pitch diameters. At more realistic loads of 6000 pounds, however, for the 100-millimeter bore size and 10 000 pounds for the 150-millimeter bore size, these extra light series bearings showed IRC for $f_o/f_i = 0.58/0.52$, at speeds of 20 000 and 15 000 rpm, respectively.

Effects of curvature on torque. -

The effects of race curvature on bearing torque are shown in figures 3 and 4. Figure 3 shows torque as a function of speed for various f_o/f_i combinations for a particular 50-millimeter geometry. The marked dependence of torque on race curvature is seen from the fact that a threefold change in torque results from a change in f_o/f_i from 0.52/0.52 to 0.58/0.52. For $f_o/f_i = 0.56/0.52$, 0.58/0.52, and 0.58/0.54 control was at the inner race over the entire speed range. For 0.58/0.56 control shifted from IRC to ORC at about 19 000 rpm, as indicated by the vertical line.

The rest of the curves are at ORC.

Examination of other data from all bore sizes confirmed the following:

- (1) ORC always occurs if $f_o \leq f_i$.
- (2) IRC occurs only if $f_o > f_i$.

The value of f_o/f_i also influences the transition speed from IRC to ORC. For a given geometry and load, increasing f_o or decreasing f_i will extend the upper limit of the speed range over which IRC occurs. For example, $f_o/f_i = 0.58/0.52$ will result in a higher transition speed than either 0.56/0.52 or 0.58/0.54.

It is interesting to note that even though spin occurs at an inner or outer race with the same curvature (but different types of control), IRC will often produce less torque than ORC. The curves for 0.58/0.52 (IRC) and 0.52/0.58 (ORC) in figure 3 illustrate this. The torque value for the 0.58/0.52 combination is lower than that for the 0.52/0.58 combination because the spin velocity of the balls for the former is less over

the speed range shown. This lower torque value for the 0.58/0.52 combination holds only up to a certain speed, however. Since torque increases more rapidly with speed during IRC than with ORC, there is a speed at which the two values are equal. For 50-millimeter bearings, this "equalization" speed was above 25 000 rpm. For 100-millimeter bearings, this speed was generally between 15 000 and 20 000 rpm, and near 10 000 rpm for the 150-millimeter size. Increasing the load (to 6000 and 10 000 lb) raised the equalization speed to above 20 000 rpm and near 15 000 rpm for the 100 and 150-millimeter bore sizes, respectively.

Figure 3 also shows that the curvature of the controlling race has little effect on torque for either type of control. The effects of the race curvature at the spinning contact on torque are shown in figure 4 for ORC. It can be seen that the decrease in torque with increased f at the inner race is uniform for all bore sizes and several load and speed combinations. The decrease in torque for f_i values from 0.52 to 0.58 is roughly 35 to 40 percent for all data examined.

Effects of initial contact angle on torque. - In general, the effects of a change in the initial contact angle from 15° to 20° were small, and so are not illustrated graphically. For 50-millimeter bearings lower torque was obtained with a higher contact angle, except for inner-race control at higher speeds (15 000 to 25 000 rpm). The changes involved were quite small, being less than 5 percent for all cases except that of IRC at low load and high speed. For this case the maximum change in torque was about 10 percent. The effects of contact angle on torque were quite variable for larger bore sizes during ORC. At most load and speed conditions an increase in the contact angle resulted in both increasing and decreasing torque, depending upon the geometry of the bearing. The changes were all small (less than 5 percent) and seemed to follow no simple pattern. For IRC with 100- and 150-millimeter bearings, increasing the contact angle caused an increase in torque for all conditions, including the higher loads of 6000 and 10 000 pounds. This increase in torque was highest (about 15 percent) near the transition speed.

Effects of number of balls on torque. - In general, the effect of increasing the number of balls was to decrease torque during ORC and increase it during IRC. An exception to this occurred for IRC at low speed for the 50-millimeter size. The effects of n were more pronounced during IRC, especially for the 100- and 150-millimeter bore sizes. For ORC, the decrease in torque due to a 30 percent increase in n was less than 10 percent for all conditions. For IRC, the torque increase was less than 10 percent for the 50-millimeter size, but as high as 20 percent for the larger bore sizes. This applied to all loads examined.

Effects of ball diameter on torque. - The effects of the ball diameter on torque are shown in figure 5. Increasing d caused an increase in torque for practically all conditions of load and speed examined. This increase of torque with d was more pronounced for IRC. For a 25 percent increase in d , the increase in torque was about 10 to 25 per-

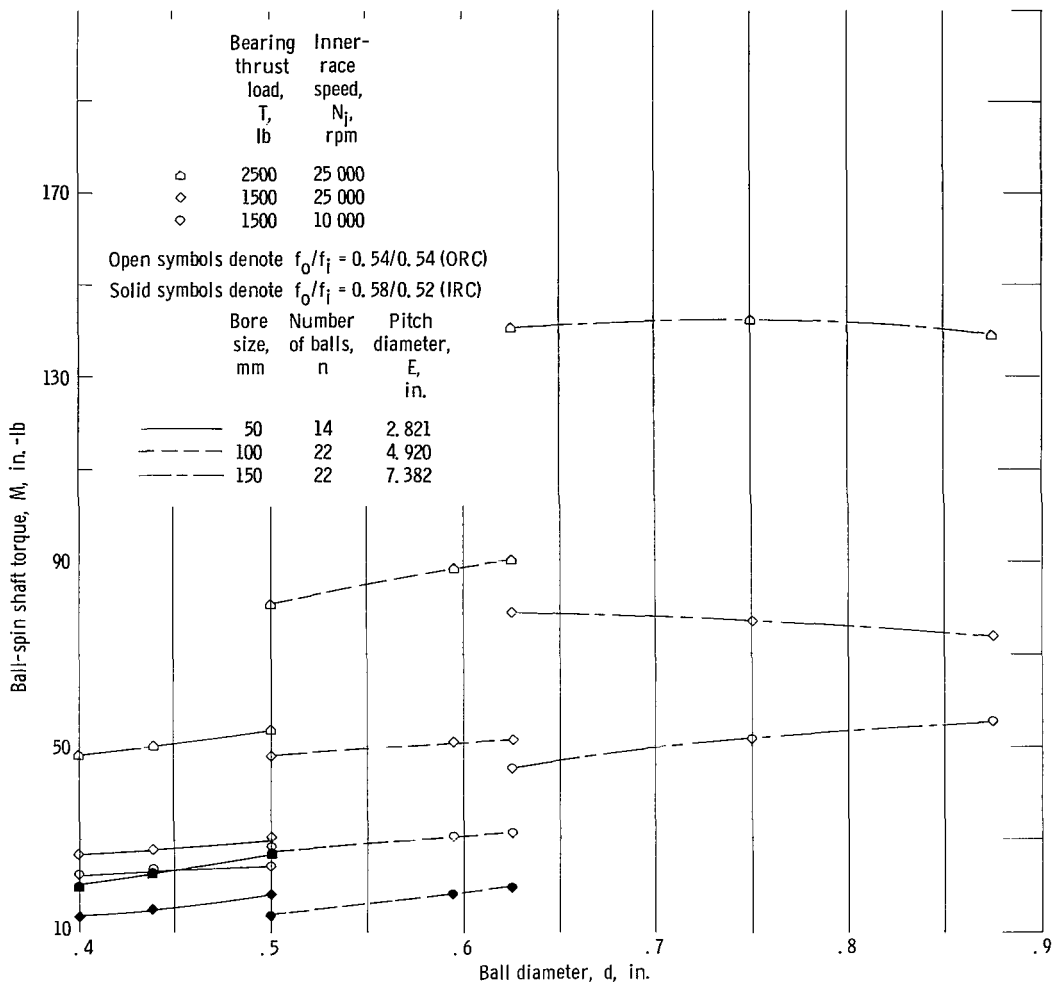
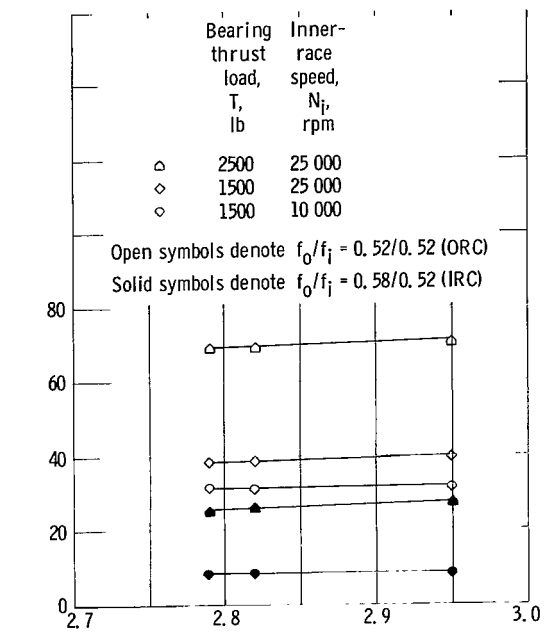


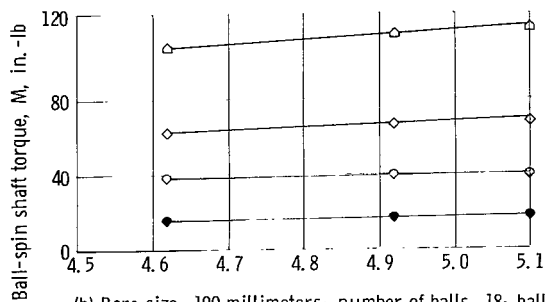
Figure 5. - Effects of ball diameter on torque. Initial contact angle (unloaded), 15° .

cent for all bore sizes at ORC and from 15 to 100 percent for IRC. The largest increases occurred near the transition speed. An exception occurred for the 150-millimeter bearings at higher speeds. Under these conditions an increase in ball diameter caused a decrease in torque, at least near the higher values of d . The decrease was most pronounced at low load (1500 lb) being about 10 percent for a 40 percent change in d . Examination of the data showed that this exception could be directly related to a decrease in the spinning velocity as d was increased.

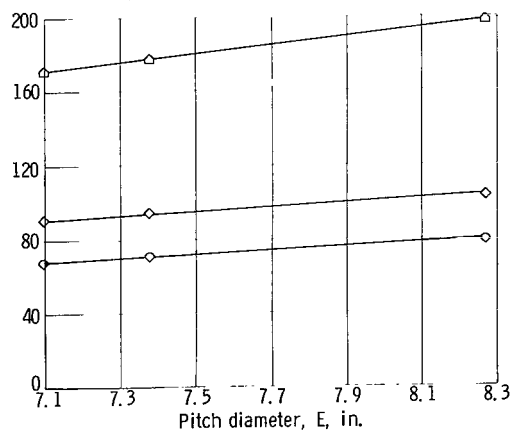
Effects of pitch diameter on torque. - The effects of a change in pitch diameter are shown in figure 6. For all loads, speeds, and geometries, increasing E resulted in increased torque. This is probably due to increased centrifugal ball loading or spin velocity. As with other parameters, the greatest effect occurred for IRC near the transition speed. A 5 percent change in E for the 50-millimeter size produced small (less than 5 percent) changes in torque during ORC, but as much as a 10 percent change during



(a) Bore size, 50 millimeters; number of balls, 12; ball diameter, 0.5 inch.



(b) Bore size, 100 millimeters; number of balls, 18; ball diameter, 0.594 inch.



(c) Bore size, 150 millimeters; number of balls, 22; ball diameter, 0.875 inch.

Figure 6. - Effects of pitch diameter on torque. Initial contact angle (unloaded), 15° .

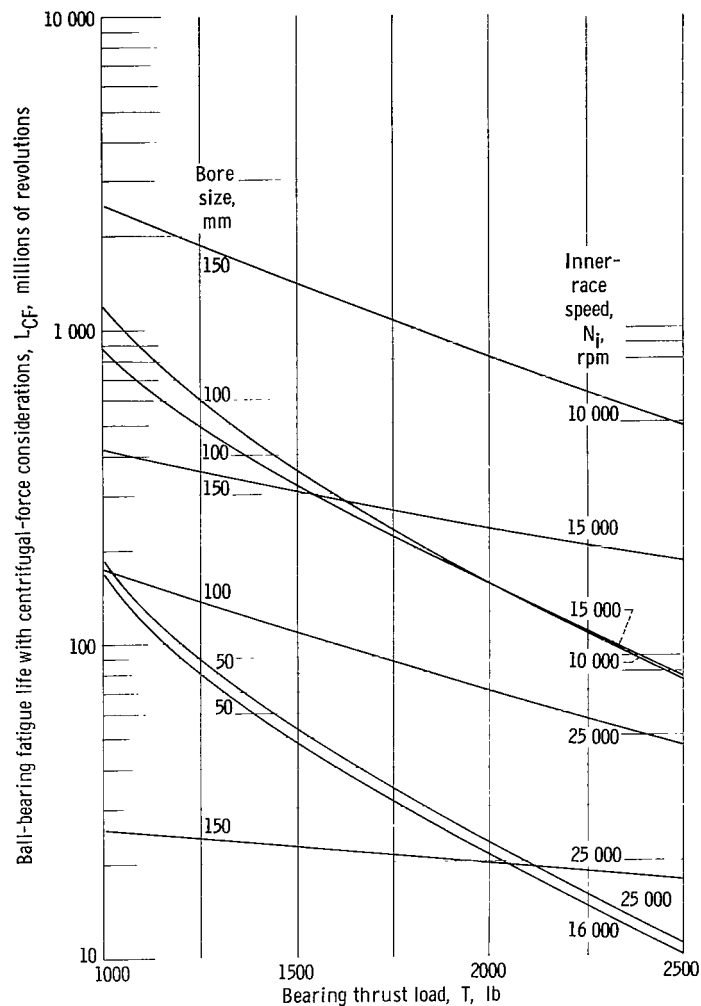


Figure 7. - Effects of load on fatigue life. Race-curvature combination, 0.52/0.52.

TABLE III. - BEARING GEOMETRIES

USED IN FIGURES 7 AND 8

[Initial contact angle (unloaded), 20°]

Bore size, mm	Number of balls, n	Ball diameter, d, in.	Pitch diameter, E, in.
50	12	0.5	2.791
100	22	.594	4.920
150	22	.875	7.382

IRC at the higher loads and speeds. For ORC, a 20 percent change in E resulted in a 5 to 10 percent change in torque for the 100-millimeter size, and a 10 to 20 percent change for the 150-millimeter size. During IRC, the change was 15 to 20 percent for the 100-millimeter size and 20 to 30 percent for the 150-millimeter size.

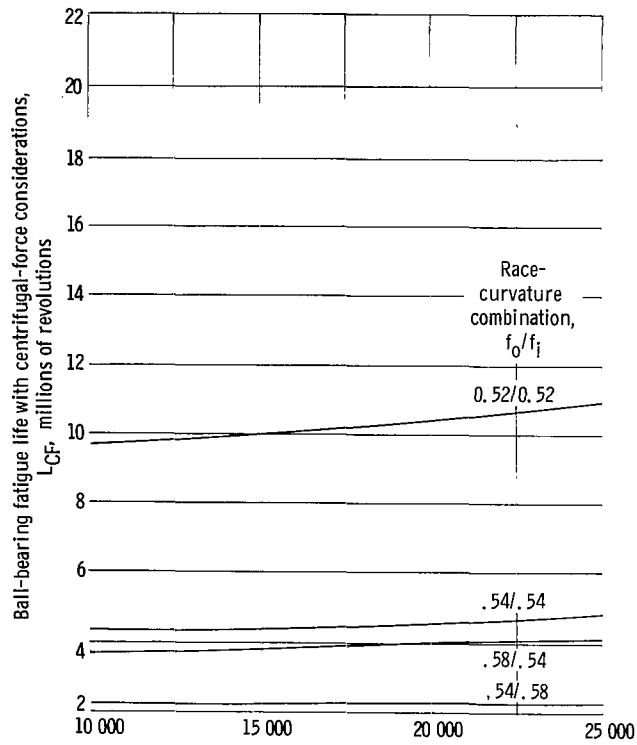
Fatigue Life

The bearing fatigue life was examined by using the Lundberg-Palmgren theory as modified by A. B. Jones to take into consideration the effects of centrifugal forces. The life of a bearing is influenced by the external or applied conditions such as thrust load and operating speed, and also by the internal design or geometry. The following design variables were examined: contact angle, race curvature, number of balls, ball diameter, and pitch diameter. The applied thrust load and operating speed were varied up to 2500 pounds and 25 000 rpm. In addition, the lives of the 100- and 150-millimeter bearings were examined at higher loads of 6000 and 10 000 pounds, respectively.

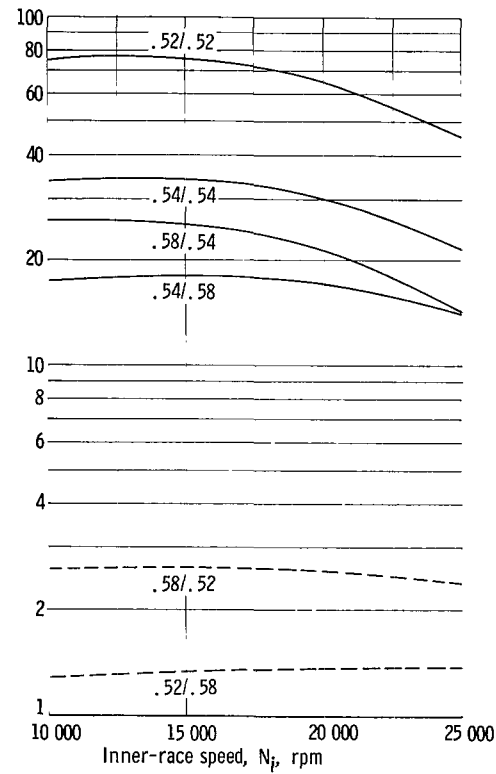
The results of the fatigue life study of the various bearings are shown on figures 7 to 12. These graphs show the fatigue life of typical designs expressed in millions of revolutions as a function of the controlled dimensions and parameters. The specific effects of each will be considered in the following sections.

Effects of load and speed on fatigue life. - The effects of load and speed on bearing fatigue life are shown in figures 7 and 8, respectively. The dimensions of these bearings are given in table III. Figure 7 shows that although increasing the load reduces life in all cases, the magnitude of the decrease depends strongly on the speed and bore size. Where centrifugal loading is high (large bore and/or high speed), the effects of thrust load are less pronounced. Figure 8 shows that the effects of speed on life are also dependent on bore size. It appears that the increase in life in the 50-millimeter size is due to a decrease in the inner-race ball load. As speed increases, the centrifugal force of the balls increases the load at the outer race. The inner-race ball load is correspondingly decreased as a result of the change in contact angles at both races. The reduction in the inner-race contact load (stress) allows a correspondingly higher number of revolutions before failure.

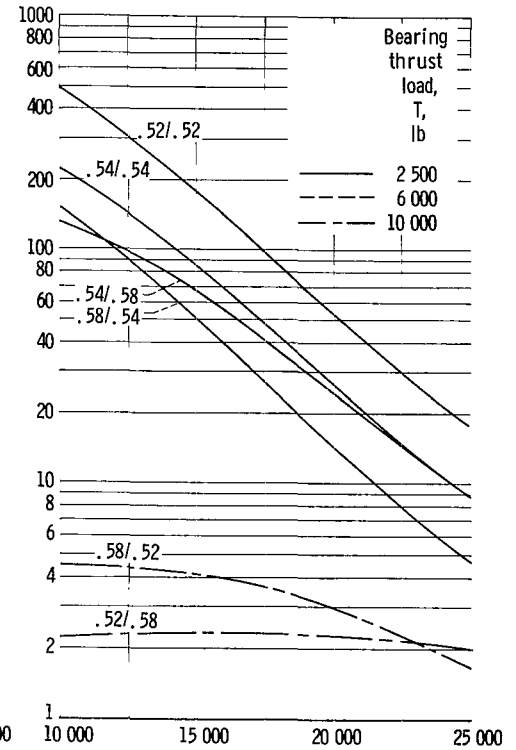
The 100- and 150-millimeter bearings show a general decreasing life pattern resulting from an increase in speed. This implies that the outer race is the determining factor of bearing life in these sizes because the increasing centrifugal forces acting on the balls, together with the changing contact angle, increase the outer-race contact stress and thereby reduce the allowable number of cycles. A speed change causes the greatest change in life when the thrust load is low. The effects of a speed change on life decrease as the thrust load is increased.



(a) Bore size, 50 millimeters.



(b) Bore size, 100 millimeters.



(c) Bore size, 150 millimeters.

Figure 8. - Effect of speed and curvature on bearing life.

Effects of geometry on fatigue life. - Figure 8 also illustrates the effects of race curvature on life. As much as a fourfold decrease in life occurs if f_o/f_i is changed from 0.52/0.52 to 0.54/0.58. The results of the calculations indicate that the life of the 50-millimeter bearing is primarily a function of the inner-race curvature. This is evident from the fact that an $f_o/f_i = 0.58/0.54$ resulted in almost twice the life as with $f_o/f_i = 0.54/0.58$. For all speeds examined, life decreased when the curvature was increased at any particular race. These results are shown in figure 8(a).

The effects of race curvature on life for the 100-millimeter size are shown in figure 8(b) for two different thrust loads. As in the case of the 50-millimeter size, the inner-race curvature is more critical than the outer one in determining life. As speed and centrifugal effects increase, however, the inner race becomes less important. This can be seen in the figure from the convergence of the two curves for 0.58/0.54 and 0.54/0.58 as speed increases at a load of 2500 pounds. At the higher load of 6000 pounds, similar results were obtained. Figure 8(b) shows that a curvature combination of 0.58/0.52 resulted in approximately twice the life of 0.52/0.58 for the extra light series bearings at this load.

The 150-millimeter bearing life is affected more by the outer-race curvature than the inner one when the load is 2500 pounds. Figure 8(c) shows that a curvature combination of 0.54/0.58 results in a higher life than 0.58/0.54 over most of the speed range.

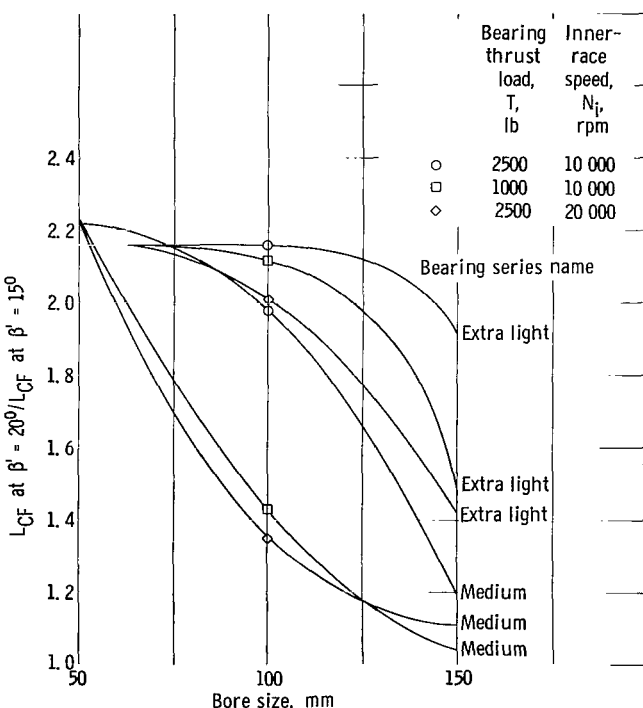


Figure 9. - Effect of contact angle on fatigue life for standard bearings. Race-curvature combination, 0.52/0.52.

At the higher load of 10 000 pounds, however, for the extra light geometries, a curvature combination of 0.58/0.52 resulted in a higher life than one of 0.52/0.58 over most of the speed range.

Figure 9 compares the life of bearings in the range from 50- to 150-millimeter bore with contact angles of 15° and 20°. The geometries used are given in table II (p. 6). The ratio of the life at 20° to the life at 15° has been plotted as a function of bore size for standard series bearings at two load and speed conditions. All data show that the life of a bearing with a 20° contact angle is greater than that of the same bearing with a 15° contact angle. The ratio of the life values varies from 1.0 to 2.3 with the larger value occurring for the 50-millimeter size.

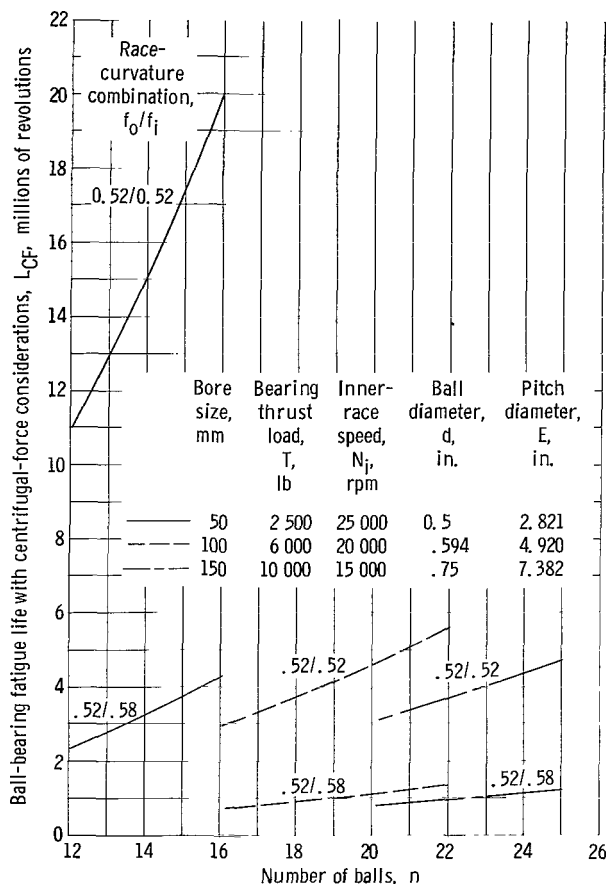


Figure 10. - Effect of the number of balls on fatigue life. Initial contact angle (unloaded), 20° .

The other parameters investigated, namely the number of balls, ball diameter, and pitch diameter, were varied separately for one thrust load at a representative speed of each bearing size. A change in any of these variables results in slightly different effects on the life of each different size bearing. These results seem to fit general trends but no definite quantitative conclusions can be made. The results of the life calculations for these variations in geometry are shown in figures 10 to 12.

Figure 10 shows the effect on bearing life for a variation in the number of balls in the rolling complement. All three bore sizes show a greatly increased life when the number of balls is increased. In general, the increase was over 100 percent for a 25 percent increase in n and was roughly the same for each bore size. Data for a 2500-pound load at these same speeds for the 100- and 150-millimeter size show similar results, although the percentage increases were not as great as with the larger loads.

Figure 11 shows the effects of a variation in ball diameter on the life of the bearings. All three sizes show an increase in life for an increase in the ball diameter. It can be seen that ball diameter has a more marked effect on life than ball number. For a 25 percent increase in d , the increase in life was about 400 percent for each bore size. A 700 percent increase is shown for the 150-millimeter bore size. As in the case of ball number, the effects of ball diameter were less pronounced at lower loads.

The effects of a change in the pitch diameter are shown in figure 12. It can be seen that the effects of E are more pronounced for larger bore sizes. For the 50-millimeter bore, almost no change was evident for the range of E examined.

The fatigue-life of a bearing is dependent upon the individual lives of its three major components: the inner race, the outer race, and the balls. Generally, the expected life of the ball exceeds the life of either race and hence is not critical. In most applications and designs, the number of stress cycles is greatest on the rotating inner race, and, therefore, this component is first to fail.

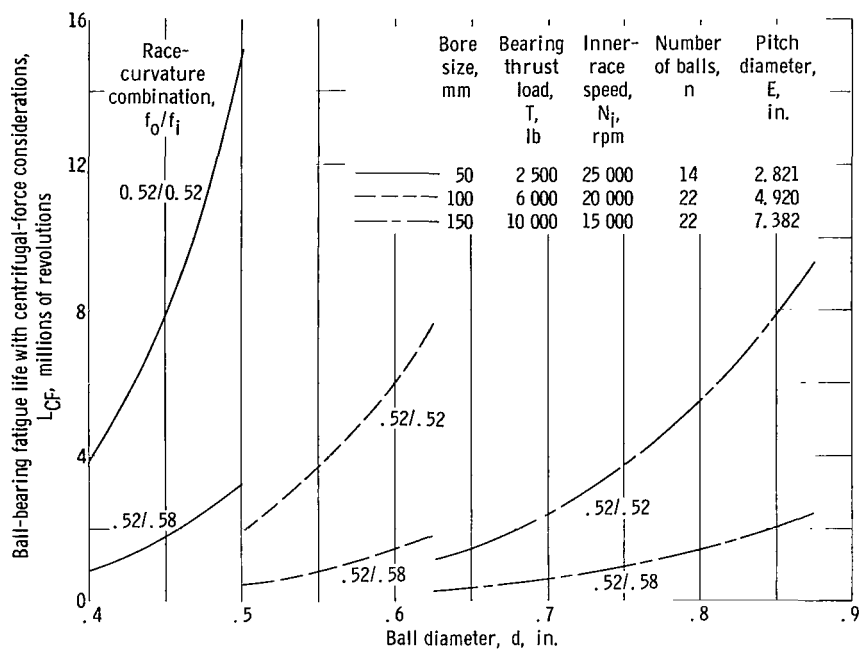


Figure 11. - Effect of ball diameter on fatigue life. Initial contact angle (unloaded), 20° .

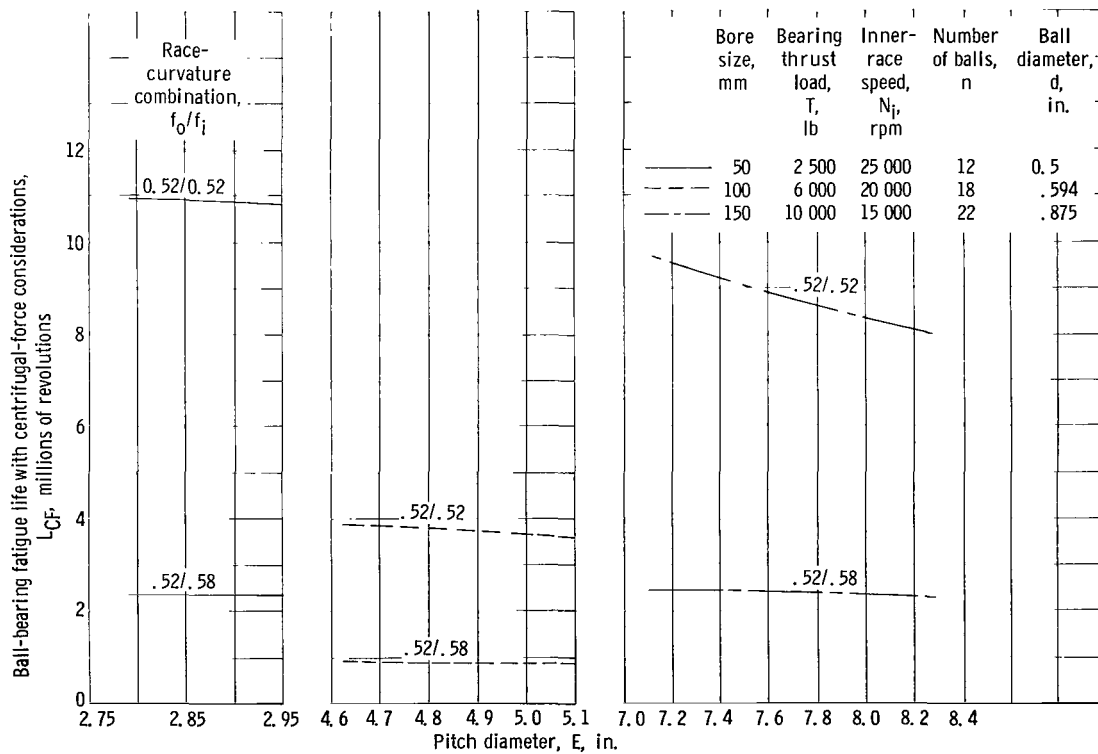


Figure 12. - Effect of pitch diameter on fatigue life. Initial contact angle (unloaded), 20° .

The stresses at the ball-race contact, for both inner and outer races, are a function of the thrust load transmitted through each ball at some operating contact angle and the centrifugal force acting on each ball (see eqs. (B5)). The inner-race ball load is directly affected only by the thrust load, but the outer-race ball load is affected by both thrust load and centrifugal force. Therefore, as the speed increases, the contact load on the outer-race increases and the inner-race load is reduced. These basic observations help explain some of the differences in the life results for the various sizes of bearings.

GEOMETRY OPTIMIZATION

From the overall results obtained, certain general rules for bearing geometry design will give an optimum bearing in that torque is minimized and life maximized. These rules are the following:

(1) The contact angle should be as large as the practical design of the bearing dictates, since a change in the contact angle has a more pronounced effect on life than on torque. The life will be increased significantly while the torque will be only slightly affected.

(2) The pitch diameter should be made as small as possible, since this simultaneously reduces torque and increases life.

(3) IRC should be utilized for bearings with bore sizes near or less than 50 millimeters. IRC is advantageous for two reasons. It generally results in less torque than ORC with reversed curvatures, and it enables the use of an arbitrarily small value of f_i , which is the more critical race curvature in determining fatigue life at typical operating speeds.

(4) ORC should be used for larger bore sizes (i. e., about 100 mm or greater). The outer-race curvature can be made small to increase fatigue life without changing torque significantly.

(5) The choice of d and n will depend largely upon the particular bore being examined; however, one generalization concerning n can be made. If ORC is to be used, n should be made as large as possible, since its effect on torque is small while its effect on life is quite significant.

SUMMARY OF RESULTS

Comparable percentage changes in the five parameters (number of balls n , ball diameter d , pitch diameter E , initial contact angle (unloaded) β^* , and race-curvature combination f_o/f_i) produced widely varying results on both the life and the ball-spin

torque. Some of the parametric changes, although large, had insignificant results, while others changed torque or life by a factor of two or more. Load and speed conditions and bore size had a large influence on the effects of many of the parametric changes. The following is a general summary of the results obtained:

1. Race curvature seemed to be the most important single variable. A change in curvature factor over the range examined (0.52 to 0.58) changed torque by a factor of three or life by a factor of four in some cases. Inner-race control (IRC) was advantageous for 50-millimeter bearings.

2. The examined change in contact angle (15° to 20°) produced negligible changes in torque (less than 5 percent) except during inner-race control near the transition speed. The effect on life was significant, especially for the 50-millimeter bore size. Increasing the angle from 15° to 20° doubled the life in this case.


3. For the change in ball number examined (25 to 35 percent), the effects on life were much greater than the effects on torque. The torque changes were in the range of 5 to 20 percent. On the other hand, life increased by over 100 percent at typical loads and speeds.

4. For a 25 to 40 percent increase in ball diameter, torque increased by as much as 100 percent for the 150-millimeter bearings. Life increased markedly with d for all conditions. At typical loads and speeds, the increase was from 400 to 700 percent.

5. A decrease in the pitch diameter caused a decrease in torque and an increase in life for all conditions examined. The effects were more pronounced for large bore size.

The following table lists the criteria for low torque and for high life for the three bore sizes at typical loads and speeds (2500 lb and 25 000 rpm for the 50-mm size, 6000 lb and 20 000 rpm for the 100-mm size, 10 000 lb and 15 000 rpm for the 150-mm size):

Criteria for-	Number of balls, n	Ball diameter, d	Pitch diameter, E	Initial contact angle (unloaded), β'	Race curvature combination, f_o/f_i
Low ball-spin torque	Small (for IRC)	Small	Small	Small (for IRC)	Large f at spinning contact
High fatigue life	Large	Large	Small	Large	Both f 's small



In spite of the opposing nature of torque and life with respect to geometry changes, a significant degree of optimization can be achieved.

Lewis Research Center,
National Aeronautics and Space Administration,
Cleveland, Ohio, February 8, 1965.

APPENDIX A

SYMBOLS

a	contact ellipse semimajor axis, in.	M_s	individual ball-spin moment, in. -lb
B	total curvature factor $f_o + f_i - 1$	N_i	inner-race speed, rpm
b	contact ellipse semiminor axis, in.	n	number of balls
C_{CF}	centrifugal-force correction factor for fatigue life	P	normal ball load, lb
d	ball diameter, in.	P_E	equivalent load (in fatigue life calculation), lb
E	pitch diameter, in.	Q	total ball-spin heat generation, Btu/min
E(k)	complete elliptic integral of the second kind, eq. (B7)	T	bearing thrust load, lb
F_c	centrifugal force on a ball, lb	$\alpha_1, \alpha_2, \left. \begin{matrix} \gamma, \Delta, \theta \end{matrix} \right\}$	angles defined in fig. 13
f	race-curvature factor expressed as ratio of race radius of curvature to ball diameter	β	operating contact angle, deg
K, K_a , K_b	various constants (ref. 8)	β'	initial contact angle (unloaded), deg
k	elliptic integral modulus, $\left[1 - (b^2/a^2)\right]^{1/2}$	β_1	static contact angle (loaded), deg
L_B	ball-bearing fatigue life without centrifugal-force considerations, millions of revolutions	μ	coefficient of sliding friction
L_{CF}	ball-bearing fatigue life with centrifugal-force considerations, millions of revolutions	ω	total angular velocity of ball about its rolling axis, rad/sec
M	shaft torque due to ball spin, in. -lb	ω_i	angular velocity of inner race, rad/sec
		ω_r	rolling component of ball angular velocity relative to race, rad/sec
		ω_s	spinning component of ball angular velocity relative to race, rad/sec
		Subscripts:	
		i	inner race
		o	outer race

APPENDIX B

EQUATIONS FOR COMPUTING BALL-SPIN TORQUE AND FATIGUE LIFE

Ball-Spin Friction Torque

Compute β_1 from reference 8

$$\frac{T}{nd^2 K} = \sin \beta_1 \left(\frac{\cos \beta_1}{\cos \beta'} - 1 \right)^{3/2} \quad (B1)$$

The centrifugal force per ball is (ref. 7)

$$F_c = 5.257 \times 10^{-7} d^3 E N_i \left(1 - \frac{d \cos \beta_1}{E} \right)^2 \quad (B2)$$

while the operating contact angles are computed from the following (ref. 7):

$$\frac{T}{nd^2} = \left[\frac{B \cos \beta' - (f_o - 0.5) \cos \beta_o - (f_i - 0.5) \cos \beta_i}{K_o \cot \beta_o (\sin \beta_o)^{1/3} + K_i \cot \beta_i (\sin \beta_i)^{1/3}} \right]^{3/2} \quad (B3)$$

and

$$\frac{nF_c}{T} = \cot \beta_o - \cot \beta_i \quad (B4)$$

The normal ball loads are given by (ref. 9)

$$\left. \begin{aligned} P_i &= \frac{T}{n \sin \beta_i} \\ P_o &= F_c \cos \beta_o + \frac{T \cos(\beta_i - \beta_o)}{n \sin \beta_i} \end{aligned} \right\} \quad (B5)$$

and

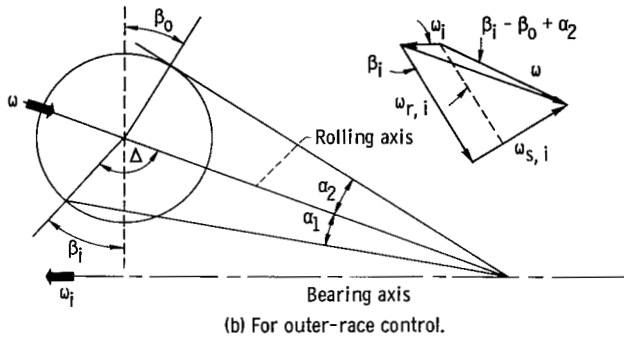
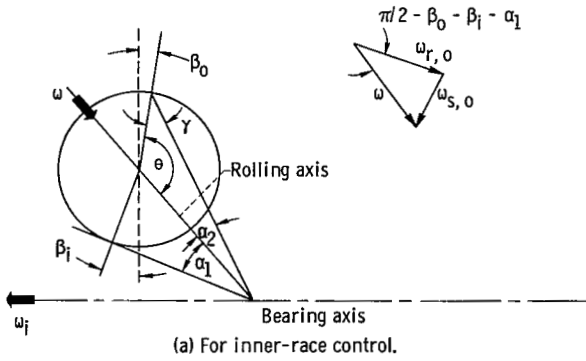


Figure 13. - Bearing geometric relations used to calculate ball-spin velocities (ref. 9).

The contact ellipse dimensions are (ref. 3)

$$\left. \begin{aligned} a &= 0.0045944 K_a (Pd)^{1/3} \\ b &= 0.0045944 K_b (Pd)^{1/3} \end{aligned} \right\} \quad (B6)$$

(The remaining equations are from ref. 9.) The individual spinning moment is given by

$$M_s = \frac{3}{8} \mu Pa E(k) \quad (B7)$$

The controlling race is that which corresponds to the larger moment. The total heat generation is then

$$\left. \begin{aligned} Q &= n \omega_{s, i} M_{s, i} \quad \text{for ORC} \\ Q &= n \omega_{s, o} M_{s, o} \quad \text{for IRC} \end{aligned} \right\} \quad (B8)$$

The ball-spin torque is

$$M = \frac{Q}{\omega_i} \quad (B9)$$

The spinning velocities $\omega_{s, i}$ and $\omega_{s, o}$ are computed from the following equations (see fig. 13):

For IRC,

$$\left. \begin{aligned}
 \tan \alpha_1 &= \frac{\sin \beta_i}{\frac{E}{d} - \cos \beta_i} \\
 \frac{1}{2} (\gamma + \alpha_2) &= \frac{1}{2} (\pi - \theta) \\
 \tan \frac{1}{2} (\gamma - \alpha_2) &= \tan \frac{1}{2} (\gamma + \alpha_2) \frac{\frac{E}{d} - \sin(\beta_i + \alpha_1)}{\frac{E}{d} + \sin(\beta_i + \alpha_1)} \\
 \alpha_2 &= \frac{1}{2} (\gamma + \alpha_2) - \frac{1}{2} (\gamma - \alpha_2) \\
 \omega &= \frac{\omega_i \sin \beta_i}{\cos \alpha_1 (\tan \alpha_1 + \tan \alpha_2)} \\
 \omega_{s, o} &= \omega \sin(\beta_i + \alpha_1 - \beta_o)
 \end{aligned} \right\} \quad (B10)$$

For ORC,

$$\left. \begin{aligned}
 \tan \alpha_2 &= \frac{\sin \beta_o}{\frac{E}{d} + \cos \beta_o} \\
 \Delta &= \frac{\pi}{2} + \beta_i - \beta_o + \alpha_2 \\
 \sin \alpha_1 &= \frac{\sin \Delta}{\left\{ 1 + \left[\frac{\frac{E}{d}}{\sin(\beta_o - \alpha_2)} \right]^2 - 2 \cos \Delta \left[\frac{\frac{E}{d}}{\sin(\beta_o - \alpha_2)} \right] \right\}^{1/2}} \\
 \omega &= \frac{\omega_i \left(\frac{E}{d} - \cos \beta_i \right)}{(\sin \alpha_1 + \cos \alpha_1 \tan \alpha_2) \left\{ 1 + \left[\frac{\frac{E}{d}}{\sin(\beta_o - \alpha_2)} \right]^2 - 2 \cos \Delta \left[\frac{\frac{E}{d}}{\sin(\beta_o - \alpha_2)} \right] \right\}^{1/2}} \\
 \omega_{s, i} &= \omega \sin(\beta_i - \beta_o + \alpha_2) + \omega_i \sin \beta_i
 \end{aligned} \right\} \quad (B11)$$

Ball-Bearing Fatigue Life

The life without centrifugal force consideration is given by (ref. 6)

$$L_B = \frac{2.44 \times 10^{10} n^2 d^{5.4} (\cos \beta')^{2.1} \left(\frac{d \cos \beta'}{E} \right)^{0.9} \left(1 - \frac{d \cos \beta'}{E} \right)^{4.17} \left(\frac{2f_i}{2f_i - 1} \right)^{1.23}}{P_E^3 \left(1 + \frac{d \cos \beta'}{E} \right) \left\{ 1 + 1.14 \left(\frac{1 - \frac{d \cos \beta'}{E}}{1 + \frac{d \cos \beta'}{E}} \right)^{5.733} \left[\frac{f_i(2f_o - 1)}{f_o(2f_i - 1)} \right]^{1.367} \right\}^{0.9}}$$

(B12)

where

$$P_E = \frac{0.4 T \cot \beta'}{1 - \frac{1}{3} \sin \beta'}$$

The correction factor for including the effects of centrifugal ball loading is given by (ref. 7)

$$C_{CF} = \frac{L_{CF}}{L_B} = \frac{\left(\frac{\sin \beta_i}{\sin \beta_o} \right)^3 \left(\frac{1 - \frac{d \cos \beta_i}{E}}{1 + \frac{d \cos \beta_i}{E}} \right)^{4.17} \left(\frac{2 + \frac{2d \cos \beta_i}{E}}{2 + \frac{d \cos \beta_o}{E} + \frac{d \cos \beta_i}{E}} \right) \left\{ 1 + \left[\frac{f_i(2f_o - 1)}{f_o(2f_i - 1)} \right]^{1.367} \left(\frac{1 - \frac{d \cos \beta_i}{E}}{1 + \frac{d \cos \beta_i}{E}} \right)^{5.733} \right\}^{0.9}}{\left\{ 1 + \frac{\sin \beta_i}{\sin \beta_o} \frac{1}{3} \left[\frac{f_i(2f_o - 1)}{f_o(2f_i - 1)} \right]^{1.367} \left(\frac{1 - \frac{d \cos \beta_i}{E}}{1 + \frac{d \cos \beta_o}{E}} \right)^{4.633} \left(\frac{2 - \frac{d \cos \beta_o}{E} - \frac{d \cos \beta_i}{E}}{2 + \frac{d \cos \beta_o}{E} + \frac{d \cos \beta_i}{E}} \right)^{1.111} \right\}^{0.9}}$$

(B13)

REFERENCES

1. Scibbe, H.W.; and Anderson, W.J.: Evaluation of Ball-Bearing Performance in Liquid Hydrogen at DN Values to 1.6 Million. ASLE Trans., vol. 5, no. 1, Apr. 1962, pp. 220-232.
2. Wong, George S.: High Pressure Pumping Technology. Rept. No. R-5155, Interim Rept., Rocketdyne Div., North Am. Aviation, Inc., May 1963.
3. Jones, A.B.: Ball Motion and Sliding Friction in Ball Bearings. J. Basic Eng. (ASME Trans.), ser. D, vol. 81, no. 1, Mar. 1959, pp. 1-12.
4. Poritsky, H.; Hewlett, C.W., Jr.; and Coleman, R.E., Jr.: Sliding Friction of Ball Bearings of the Pivot Type. J. Appl. Mech., vol. 14, no. 4, Dec. 1947, pp. A261-A268.
5. Reichenbach, G.S.: The Importance of Spinning Friction in Thrust-Carrying Ball Bearings. J. Basic Eng. (ASME Trans.), ser. D, vol. 82, no. 2, June 1960, pp. 295-301.
6. Palmgren, A.: Ball and Roller Bearing Engineering. Third ed., SKF Industries Inc., 1959.
7. Jones, A.B.: The Life of High-Speed Ball Bearings. ASME Trans., vol. 74, no. 5, July 1952, pp. 695-703.
8. Jones, A.B.: Analysis of Stresses and Deflections. Vol. 1. New Departure, Div. of General Motors Corp. (Bristol, Conn.), 1946.
9. Bisson, Edmond E.; and Anderson, William J.: Advanced Bearing Technology. NASA SP-38, 1964.

2/22/85
057

"The aeronautical and space activities of the United States shall be conducted so as to contribute . . . to the expansion of human knowledge of phenomena in the atmosphere and space. The Administration shall provide for the widest practicable and appropriate dissemination of information concerning its activities and the results thereof."

—NATIONAL AERONAUTICS AND SPACE ACT OF 1958

NASA SCIENTIFIC AND TECHNICAL PUBLICATIONS

TECHNICAL REPORTS: Scientific and technical information considered important, complete, and a lasting contribution to existing knowledge.

TECHNICAL NOTES: Information less broad in scope but nevertheless of importance as a contribution to existing knowledge.

TECHNICAL MEMORANDUMS: Information receiving limited distribution because of preliminary data, security classification, or other reasons.

CONTRACTOR REPORTS: Technical information generated in connection with a NASA contract or grant and released under NASA auspices.

TECHNICAL TRANSLATIONS: Information published in a foreign language considered to merit NASA distribution in English.

TECHNICAL REPRINTS: Information derived from NASA activities and initially published in the form of journal articles.

SPECIAL PUBLICATIONS: Information derived from or of value to NASA activities but not necessarily reporting the results of individual NASA-programmed scientific efforts. Publications include conference proceedings, monographs, data compilations, handbooks, sourcebooks, and special bibliographies.

Details on the availability of these publications may be obtained from:

SCIENTIFIC AND TECHNICAL INFORMATION DIVISION
NATIONAL AERONAUTICS AND SPACE ADMINISTRATION
Washington, D.C. 20546